Journal of Molecular Structure 1022 (2012) 211–219

Contents lists available at SciVerse ScienceDirect

Journal of Molecular Structure

journal homepage: www.elsevier.com/locate/molstruc

Experimental and theoretical study on the reaction of N^3-phenyl-(pyridin-2-yl)carbohydrazonamide with itaconic anhydride

Bożena Modzelewska-Banachiewicz [a], Renata Paprocka [a], Liliana Mazur [b], Jarosław Saczewski [c,*], Jolanta Kutkowska [d], Dorota K. Stępień [e], Michał Cyrański [e]

[a] Department of Organic Chemistry, Faculty of Pharmacy, Nicolaus Copernicus University, Jurasza 2, 85-089 Bydgoszcz, Poland
[b] Department of General and Coordination Chemistry, Maria Curie-Sklodowska University, M. Curie-Sklodowska Sq. 2, 20-031 Lublin, Poland
[c] Department of Chemical Technology of Drugs, Medical University of Gdansk, Hallera 107, 80-416 Gdansk, Poland
[d] Department of Genetics and Microbiology, Maria Curie-Sklodowska University, Akademicka 19, 20-033 Lublin, Poland
[e] Department of Chemistry, University of Warsaw, Pasteura 1, 02-093 Warsaw, Poland

HIGHLIGHTS

- New isomeric 1,2,4-triazole-containing alkenoic acids are obtained.
- Mechanisms of base-catalyzed and neutral thermal 1,3-proton shifts are studied theoretically.
- The structures are confirmed by 1D and 2D NMR and single crystal X-ray diffraction analysis.
- Antimicrobial activity of the 1,2,4-triazole-containing alkenoic acids are investigated.

ARTICLE INFO

Article history:
Received 3 March 2012
Received in revised form 24 April 2012
Accepted 25 April 2012
Available online 8 May 2012

Keywords:
1,2,4-Triazole
Carbohydrazonamide
Itaconic anhydride
Alkenoic acids
1,3-Proton shift reaction
X-ray diffraction analysis

ABSTRACT

Two new 1,2,4-triazole-containing alkenoic acid derivatives were obtained from the reaction of *N*-phenyl-(pyridin-2-yl)carbohydrazonamide with itaconic anhydride, depending on the reaction conditions. The structures of 2-((4-phenyl-5-(pyridin-2-yl)-4*H*-1,2,4-triazol-3-yl)methyl)acrylic acid or (*E*)-2-methyl-3(4-phenyl-5-(pyridine-2-yl)-4*H*-1,2,4-triazol-3-yl)acrylic acid were confirmed by means of 1D and 2D NMR spectroscopic data as well as by single-crystal X-ray diffraction analysis. The experiential ^{1}H and ^{13}C chemical shifts were compared with those calculated with B3LYP, EDF1, and EDF2 density functional theories. The theoretical study of the observed terminal-to-internal alkene isomerization was performed with density functional (DFT) B3LYP/6-31+G* method using SM8 water and DMF solvation models. Antimicrobial activities of the newly prepared alkenoic acid derivatives were verified experimentally by a broth microdilution method.

1. Introduction

1,2,4-Triazole derivatives constitute an important class of heterocyclic compounds, which gained considerable attention in recent years due to a broad spectrum of biological properties, which include: antimicrobial, antiviral, anticancer, antiasthmatic, anticonvulsant, antidepressant, antihypertensive, antiemetic, hypnotic, sedative, anxiolytic, antithyroid, hypoglycemic and antimigraine activity [1]. Among them fluconazole and itraconazole belong to the most powerful antimycotic drugs used today in the treatment and prevention of superficial and systemic fungal infections. On the other hand, it is well known that derivatives of various alkenoic acids [2–4] and cinnamic acid [5] exhibit a pronounced antibacterial and antifungal activities.

In view of the above, we expected that by combining the 1,2,4-triazole ring system and the alkenoic acid moiety, a new class of heterocyclic analogues of cinnamic acid with the desired antimicrobial properties could be obtained. Our research plane aimed at achieving that goal was based on previous investigations of hydrazonamide chemistry [6–9] and chemical properties of itaconic anhydride [10,11]. The synthetic pathways leading to 2-((4-phenyl-5-(pyridin-2-yl)-4*H*-1,2,4-triazol-3-yl)methyl)acrylic acid (**3**) and (*E*)-2-methyl-3(4-phenyl-5-(pyridine-2-yl)-4*H*-1,2,4-triazol-3-yl)acrylic acid (**4**) are presented in Scheme 1. The molecular structures of alkenoic acid derivatives obtained were confirmed

* Corresponding author. Tel.: +48 583491953; fax: +48 583491654.
E-mail address: js@gumed.edu.pl (J. Saczewski).

0022-2860/$ - see front matter © 2012 Elsevier B.V. All rights reserved.
http://dx.doi.org/10.1016/j.molstruc.2012.04.087

by 1D and 2D NMR spectral data and single crystal X-ray diffraction analysis. Moreover, a facile isomerization of the terminal alkene derivative into the more thermodynamically stable internal alkene prompted us to investigate the mechanisms of both the base-catalyzed and the thermal 1,3-proton shifts using DFT B3LYP/6-31+G* method combined with SM8 (H_2O, DMF) solvation models.

2. Experimental

2.1. Materials and methods

Chemicals were purchased from Aldrich and used without further purification. Melting points were measured on a Mel TEMP 1002D apparatus and are uncorrected. Mass spectra data were obtained on Finingan Trace DSQ GC/MS with electrospray ion source. The FT-IR spectra were recorded from KBr pellets in the range of 4000–400 cm^{-1} on Perkin Elmer Spectrum 2000 infrared spectrometer. The elemental analysis was made with a Vario Macro 11.45-0000 (Elementar Analysesysteme GmbH, Germany) operating with the software VARIOEL. ^1H NMR and ^{13}C NMR spectra were recorded on a Bruker Avance spectrometer in DMSO-d_6 with TMS as an internal standard. N^3-phenyl-(pyridine-2-yl)carbohydrazonamide (**1**) was synthesized according to the previously described procedure [6].

2.2. Synthesis of 2-((4-phenyl-5-(pyridin-2-yl)-4H-1,2,4-triazol-3-yl)methyl)acrylic acid (*3*)

The carbohydrazonamide **1** (2.12 g, 10 mmol) and itaconic anhydride **2** (1.12 g, 10 mmol) were dissolved in anhydrous diethyl ether (50 mL) and the reaction mixture was left at room temperature for 7 days. The solid product that precipitated was collected by filtration and washed with diethyl ether. Then, the solid was dissolved in chloroform (30 mL), heated at reflux for 5 min. and filtered. The filtrate was evaporated to dryness and the solid residue was washed with anhydrous diethyl ether, dried and purified by crystallization from water to give 0.46 g (1.5 mmol, 15%) of **3**.

M.p. 164–166 °C. ^1H NMR (300 MHz, DMSO-d_6): δ = 3.56 (s, 2 H, CH_2), 5.58 (s, 1 H, CH), 6.13 (s, 1 H, CH), 7.30–7.37 (m, 3 H, CH), 7.45–7.48 (m, 3 H, CH), 7.89 (t, J = 6,0 Hz, 1 H, CH), 7.96 (d, J = 6.0 Hz, 1H, CH), 8.29 (d, J = 6.0 Hz, 1 H, CH), 12.59 (bs, 1 H, COOH) ppm. ^{13}C NMR (100 MHz, DMSO-d_6): δ = 29.3, 125.5, 126.0, 128.7, 129.2, 130.9, 131.0, 136.9, 137.9, 139.0, 148.5, 150.7, 154.3, 155.8, 168.9. FT-IR (KBr, cm^{-1}): 3426m, 3078m, 1711s, 1635m, 1591m, 1500s, 1457s, 1417m, 1218m, 1164m, 1008m, 954w, 792m, 781m, 700m. ESI-MS m/z (%): 306 (57%), 261 (100%), 130 (28%), 78 (41%), 77 (50%). Anal. Calc. for $C_{17}H_{14}N_4O_2$: C, 66.66; H, 4.61; N, 18.29%; found: C, 66.46; H, 4.62; N, 18.07%.

2.3. Isomerization of *3* to (E)-2-methyl-3-(4-phenyl-5-(pyridin-2-yl)-4H-1,2,4-triazol-3-yl)acrylic acid (*4*)

Method I: Compound **3** (0.46 g, 1.5 mmol) was dissolved in 2% aqueous solution of sodium hydroxide (10 mL) and the reaction mixture was left at room temperature for 12 h. Then, the solution was cooled to room temperature and neutralized with 1% hydrochloric acid. The precipitate thus obtained was collected by filtration, washed with water and dried in vacuum to give 0.44 g (1.4 mmol, 95.6%) of **4**.

Method II: Compound **3** (0.46 g, 1.5 mmol) was dissolved in dimethylformamide (10 mL) and heated at 150 °C for 4 h. Upon cooling to room temperature the reaction mixture was filtered and the filtrate was diluted with water (10 mL). The product that precipitated was collected by filtration, washed with water and dried in vacuum to yield 0.27 g (0.88 mmol, 58.7%) of **4**.

M.p. 234–236 °C. ^1H NMR (500 MHz, DMSO-d_6): δ = 2.42 (d, ^3H, CH_3, J = 1.5 Hz); 6.85 (d, ^1H, CH, J = 1.5 Hz); 7.36–7.41 (m, ^3H, CH); 7.49–7.54 (m, ^3H, CH); 7.92 (t, J = 7.9 Hz, ^1H, CH); 8.04 (d, J = 7.9 Hz, ^1H, CH); 8.30–8.32 (m, ^1H, CH); 12.8 (s, ^1H, COOH). ^{13}C NMR (125 MHz, DMSO-d_6): δ = 15.2, 119.0, 124.0, 124.5, 127.8, 129.4, 129.5, 134.5, 136.0, 137.2, 146.2, 149.1, 152.4, 152.5, 168.2. FT-IR (KBr, cm^{-1}): 3428s, 3055m, 2923w, 2496w, 1938w, 1704s,

Table 1
Experimental and DFT B3LYP/6-31+G* ^1H and ^{13}C NMR chemical shifts δ of **3** and **4** with the root-mean-square deviation (RMSD).

H, or C atom atom	Chemical shift δ experimental	B3LYP/6-31+G* calculated	B3LYP/6-31+G* corrected[a]	EDF1	EDF2
3					
C—4H_2	3.56	3.06		3.26	3.12
C—6H	5.58	5.95		6.04	5.99
C—6H′	6.13	6.45		6.49	6.51
RMSD		0.40		0.38	0.41
4					
C—12H_3	2.42	2.64		2.82	2.69
C—22H	6.85	6.60		6.59	6.70
C—3PH	8.04	8.68		8.73	8.74
C—4PH	7.92	7.49		7.49	7.51
C—5PH	7.38	6.80		6.79	6.82
C—6PH	8.31	8.04		8.15	8.05
RMSD		0.43		0.46	0.43
C-12	15.2	16.4	16.14	19.2	16.5
C-22	119.0	116.7	122.8	114.5	116.9
C-2	136.0	130.0	136.0	128.7	130.3
C-1	168.3	157.0	168.9	154.7	156.9
C-3	152.5	146.5	156.4	144.8	146.2
C-5	152.4	148.9	158.8	147.1	148.7
C—2P	146.2	141.9	151.3	139.6	141.5
C—3P	124.1	118.0	124.1	116.5	118.3
C—4P	137.3	128.7	135.0	125.9	128.9
C—5P	124.5	116.1	122.7	114.2	116.5
C—6P	149.1	141.3	151.0	139.5	141.5
RMSD		6.60	3.16	8.48	6.54

[a] The corrected ^{13}C chemical shifts account local environment in addition to directly calculated shifts.

1644m, 1498s, 1440s, 1295s, 1241s, 992m, 793m, 774s, 696m, 586m. ESI-MS *m/z* (%): 306 (85%), 288 (24%), 261 (100%), 156 (32%), 130 (69%), 78 (67%), 77 (87%). Anal. Calc. for $C_{17}H_{16}N_4O_3$: C, 62.95; H, 4.97; N, 17.27%; found: C, 62.86; H, 5.12; N, 16.89%.

2.4. Synthesis of (E)-2-methyl-3-(4-phenyl-5-(pyridin-2-yl)-4H-1,2,4-triazol-3-yl)acrylic acid (**4**)

A solution of hydrazonamide **1** (2.12 g, 10 mmol) and itaconic anhydride (**2**) (1.12 g, 10 mmol) in anhydrous diethyl ether (50 mL) was stirred vigorously at room temperature for 2 h. The solid that precipitated was collected by filtration, washed with diethyl ether and dried under vacuum. Then, the dry solid thus obtained was dissolved in 2% aqueous NaOH solution and the reaction mixture was heated under reflux for 2 h. Upon cooling to room temperature the solution was neutralized with 1% HCl. The solid that precipitated was collected by filtration, washed with water and dried in vacuum to give 2.32 g (7.57 mmol, 75%) of **4**.

2.5. X-ray structure analysis

Single-crystals of **3** and **4** suitable for X-ray analysis, were obtained by slow crystallization from ethanol. The XRD measurements for **3** and **4** were performed at 100 K on Oxford Diffraction Xcalibur CCD diffractometer with the graphite-monochromatized Mo Kα radiation and Gemini κ-axis diffractometer with graphite-monochromated Enhance Cu Kα radiation, respectively. The crystals were positioned at 55 mm from the CCD camera. Data sets were collected using the ω scan technique, with an angular scan width of 0.75° and 1.0° for **3** and **4**, respectively. In both cases the data were corrected for Lorentz and polarization effects. Multi-scan absorption correction was also applied [12]. Data reduction and analysis were carried out with the CrysAlis RED, Oxford Diffraction Ltd. [13]. The structures were solved by direct methods [14] and refined using SHELXL [15]. The refinement was based on F^2 for all reflections except those with very negative F^2. The weighted *R* factors *wR* and all goodness-of-fit *S* values are based on F^2. The non-hydrogen atoms were refined anisotropically. In **3** the H atoms adjacent to O1 and C6 atoms were found in the difference-Fourier maps and refined with isotropic displacement parameters. All remaining H atoms were positioned geometrically [C—H = 0.97 Å for CH_2 and 0.93 Å for $CH_{(ar)}$] and refined using the riding model with $U_{iso}(H) = 1.2U_{eq}(C)$. In **4** all hydrogen atoms were located from a difference Fourier map; their positions and thermal parameters were refined isotropically. The scattering factors were taken from Tables 6.1.1.4 and 4.2.4.2 [16].

All figures presenting the results of X-ray diffraction determination were made using the MERCURY program [17]. Crystal data and structural refinement for **3** and **4** are specified in Table 2. Selected bond lengths, bond angles, major torsion angles and hydrogen bonds are given in Tables 3 and 4. Displacement ellipsoids and atom numbering are shown in Figs. 1 and 2, respectively. Packing and hydrogen bonds are shown in Figs. 3–6.

Table 2
Crystal data and structure refinement details for **3** and **4**.

	3	**4**
Formula	$C_{17}H_{14}N_4O_2$	$C_{17}H_{16}N_4O_3$
Formula weight (g mol^{-1})	306.32	324.34
T (K)	100(2)	100(2)
Wavelength (Å)	0.71073	1.54184
Crystal system, space group	Monoclinic, $P2_1/n$	Monoclinic, *Pn*
a (Å)	9.1499(3)	5.8875(2)
b (Å)	10.0043(3)	8.5996(3)
c (Å)	16.2523(7)	15.7666(6)
β (°)	104.686(4)	96.743(4)
V (Å^3)	1439.10(9)	792.74(5)
Z	4	2
Calculated density (g cm^{-3})	1.414	1.359
θ Range (°)	3.56–28.28	5.14–67.08
Absorption coefficient (mm^{-1})	0.097	0.793
Crystal size (mm)	0.49 × 0.25 × 0.16	0.31 × 0.23 × 0.11
Crystal color and form	Colorless prism	Colorless prism
Reflections collected/unique	21461/3556 [R_{int} = 0.059]	8777/2706 [R_{int} = 0.041]
Observed reflections ($I > 2\sigma(I)$)	2463	2551
Data/restraints/parameters	3556/0/220	2706/2/279
Final *R* indices ($I > 2\sigma(I)$)	R_1 = 0.0403; wR_2 = 0.0914	R_1 = 0.0332; wR_2 = 0. 0803
R indices (all data)	R_1 = 0.0664; wR_2 = 0.0984	R_1 = 0.0359; wR_2 = 0.0816
Goodness-of-fit on F^2	0.923	1.026
Completeness to *θ* max. (%)	99.7	99.9
Largest diff. peak and hole (e Å^{-3})	0.31/−0.21	0.13/−0.21

Table 3
Selected geometric parameters.

	3	**4**
Bond distances (Å)		
C1—O1	1.326(2)	1.315(3)
C1—O2	1.213(2)	1.220(2)
C1—C2	1.493(2)	1.497(3)
C2—C6	1.315(2)	1.494(3)
C2—C4	1.505(2)	1.345(3)
C3—C4	1.498(2)	1.454(3)
N1—N2	1.383(2)	1.380(2)
N2—C3	1.307(2)	1.318(3)
C3—N4	1.374(2)	1.377(2)
N4—C5	1.375(2)	1.373(2)
C5—N1	1.315(2)	1.311(2)
Bond angles (°)		
O2—C1—O1	124.2(1)	123.5(2)
O2—C1—C2	123.1(1)	124.1(2)
O1—C1—C2	112.7(1)	112.4(2)
Torsion angles (°)		
O1—C1—C2—C4	160.0(1)	−150.7(2)
O1—C1—C2—C6	−25.4(2)	28.4(2)
C1—C2—C4—C3	−59.5(2)	179.2(2)
C6—C2—C4—C3	126.1 (2)	0.2(3)
C2—C4—C3—N2	−13.1(2)	19.9(3)

Table 4
Geometry of proposed hydrogen bonds for **3** and **4**.

	D—H (Å)	H···A (Å)	D···A (Å)	<D—H···A (°)
3				
O1—H1o···N3$^{(i)}$	1.00(2)	1.74(3)	2.705(3)	164(3)
C11—H11···O2$^{(ii)}$	0.93	2.63	3.342(3)	134
C6—H6a···O1$^{(iii)}$	1.03(2)	2.66(2)	3.411(3)	127(3)
C6—H6b···N1$^{(iv)}$	1.04(2)	2.69(2)	3.590(2)	149(2)
C14—H14···N1$^{(v)}$	0.93	2.54	3.412(2)	157
C8—H8···N1$^{(vi)}$	0.93	2.46	3.318(3)	154
4				
O1w—H1w···O2	0.81(3)	2.02(3)	2.820(2)	173(2)
O1w—H2w···N1$^{(vii)}$	0.88(3)	1.90(3)	2.780(2)	178(3)
O1w—H2w···N2$^{(vii)}$	0.88(3)	2.49(3)	3.262(2)	146(3)
O1—H1···O1w$^{(ii)}$	0.94(3)	1.59(3)	2.515(2)	167(3)
C8—H8···O2$^{(viii)}$	0.94(2)	2.47(3)	3.230(2)	138(2)
C6—H62···N3$^{(ix)}$	0.98(3)	2.60(3)	3.503(3)	155(2)

Symmetry codes: (i) $x-1, y, z$; (ii) $1+x, y, z$; (iii) $-x, -y, -z$; (iv) $1-x, -y, -z$; (v) $1/2+x, 1/2-y, 1/2+z$; (vi) $1-x, 1-y, -z$; (vii) $x, y-1, z$; (viii) $x-1, 1+y, z$; (ix) $1/2+x, 2-y, z-1/2$.

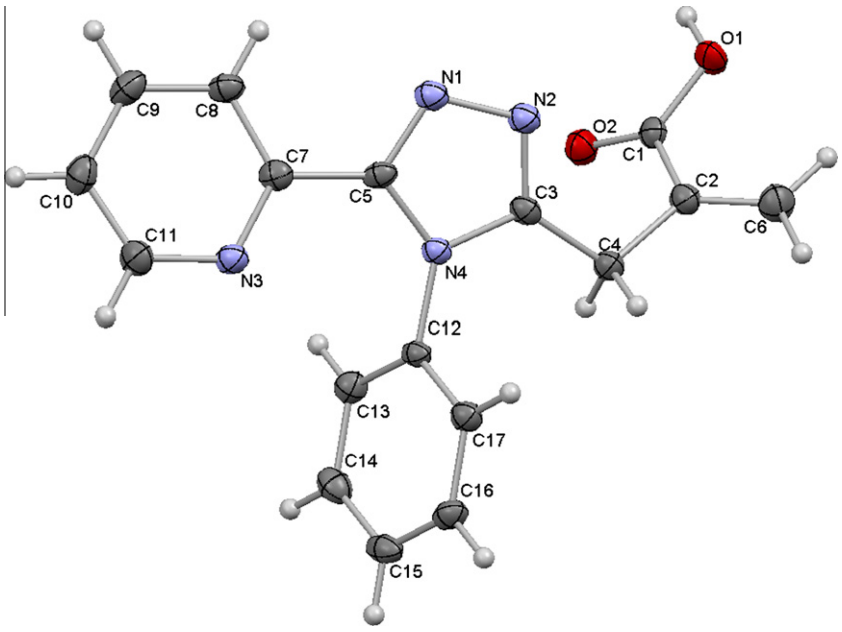

Fig. 1. The molecular structure of **3** showing the atom-numbering scheme. Displacement ellipsoids are drawn at the 50% probability level.

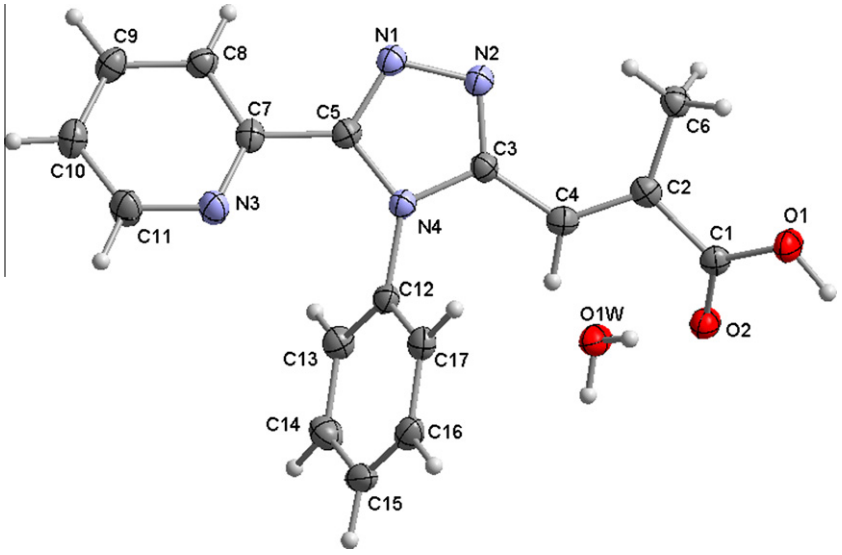

Fig. 2. Molecular structure and atomic numbering for **4**. Displacement ellipsoids are drawn at 50% probability level.

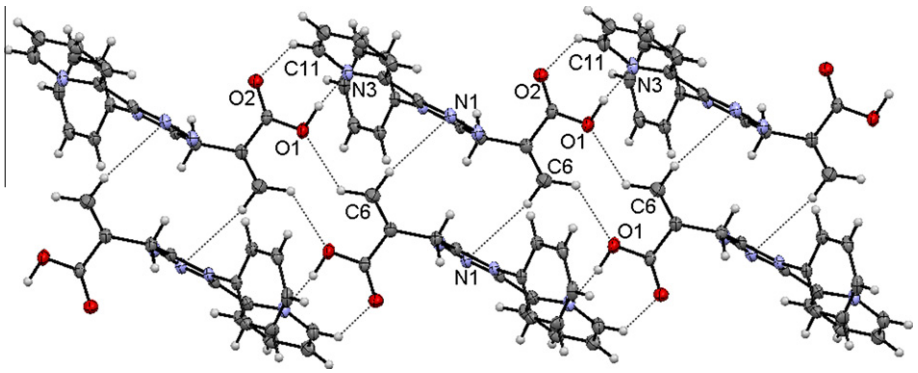

Fig. 3. Part of the crystal structure of **3**, showing hydrogen-bonded (dashed lines) molecular chains.

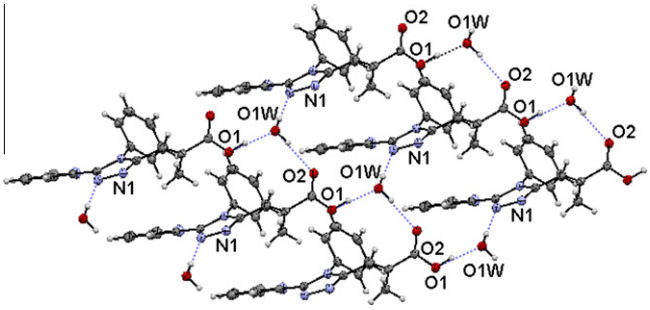

Fig. 4. Part of the crystal structure of **4**, showing hydrogen-bonded (dashed lines) molecular chains.

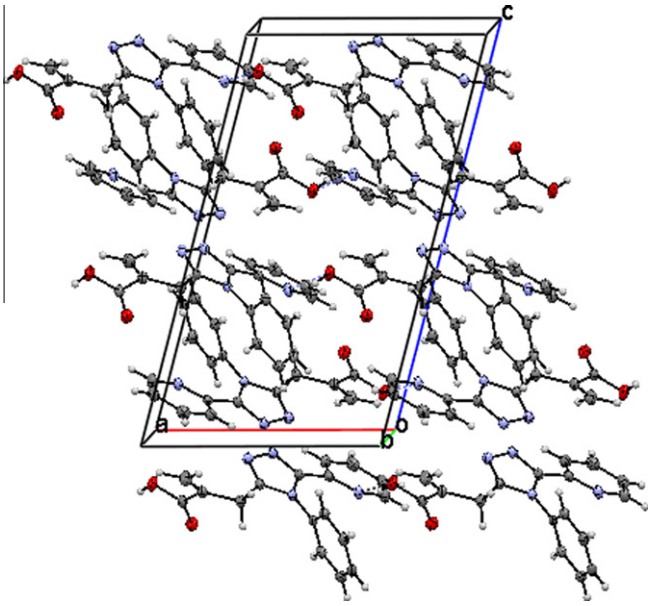

Fig. 5. Packing view of **3** along [010] direction.

2.6. Theoretical calculations

All the quantum-chemical calculations were carried out with use of the Spartan 08 program package provided by Wavefunction, Inc. [18]. The geometries were fully optimized in vacuum with DFT B3LYP method using 6-31+G* basis set combined with water SM8 solvation model [19]. Frequency calculations were performed for all structures to prove the energy minima. The Gibbs free energies were obtained from the electronic energies corrected with the zero-point energies (ZPE), thermal energies involving temperature increase from 0 to 298.15 or 423.15 K and entropies. The relative energies were obtained by subtracting the energy of the starting structures from the energies of all the other geometries and converting these differences into kcal/mol. Vibrational frequency analyses and IRC calculations were performed for all found transition states (**TSs**) to prove that they assuredly connect the reactants and products.

2.7. Antibacterial in vitro activity of compounds *3* and *4*

The susceptibility to the new synthesized compounds was determined by a broth microdilution method in standard 96-well sterile flat-bottom polystyrene plates (Kartell). The following strains were tested: Gram-negative bacteria: *Escherichia coli* ATCC 25922, *Pseudomonas aeruginosa* ATCC 27853, *Yersinia enterocolitica* O3; Gram-positive: *Staphylococcus aureus* ATCC 25923, *Enterococcus faecalis* ATCC 29212, *Sarcina lutea*; *Mycobacterium smegmatis*, *Nocardia spp*, and the pathogenic fungus *Candida albicans.* Bacterial cultures were grown on liquid Luria–Bertani (LB) medium at temperature 37 °C. The minimum inhibitory concentration (MIC_{50}) was measured by replicating 10^5 CFU/mL onto microplates supplemented with 50, 75, 100, and 250 μg/mL of corresponding compound dissolved in dimethylsulfoxide (DMSO). Tests were performed in triplicate for each concentration, in all the tests, DMSO was used as the control. After 18 h the growth of bacteria was estimated spectrophotometrically (550 nm) with an ELISA detector.

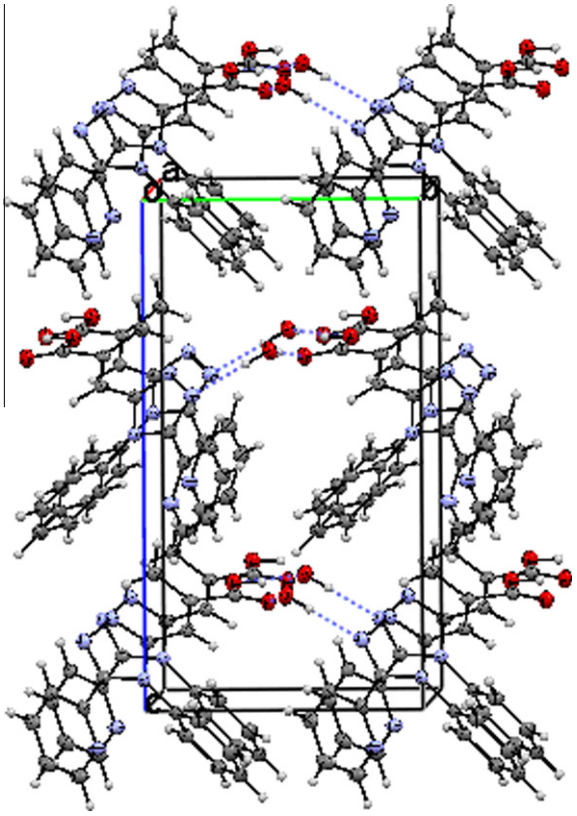

Fig. 6. Packing view of **4** along [100] direction. Dashed lines indicate hydrogen bonds.

3. Results and discussion

3.1. Synthesis

It is known that itaconic anhydride easily isomerizes to citraconic anhydride in the presence of organic bases such as pyridine or *N*,*N*-dimethylaniline [10,11]. As shown in Scheme 2, this isomerization proceeds via anionic intermediate which is stabilized in polar solvents. Therefore, to secure the formation of the final product with external C=C double bond, we have run the reaction of anhydride **1** with carbohydrazonamide **2** in diethyl ether at room temperature (Scheme 1). 2-((4-Phenyl-5-(pyridin-2-yl)-4*H*-1,2,4-triazol-3-yl)methyl)acrylic acid (**3**) thus obtained was further transformed into a more thermodynamically stable (*E*)-2-methyl-3-(4-phenyl-5-(pyridin-2-yl)-4H-1,2,4-triazol-3-yl)acrylic acid (**4**) by the treatment with aqueous 2% NaOH solution at room temperature for 12 h (base-catalyzed isomerization, 95% yield) or by heating in wet DMF at 150°C for 4 h (thermal isomerization, 58% yield).

It should be pointed out that the compound **3** incorporating terminal C=C double bond was separated in pure form in rather low yield (15%) and attempts in optimization of the synthetic procedure

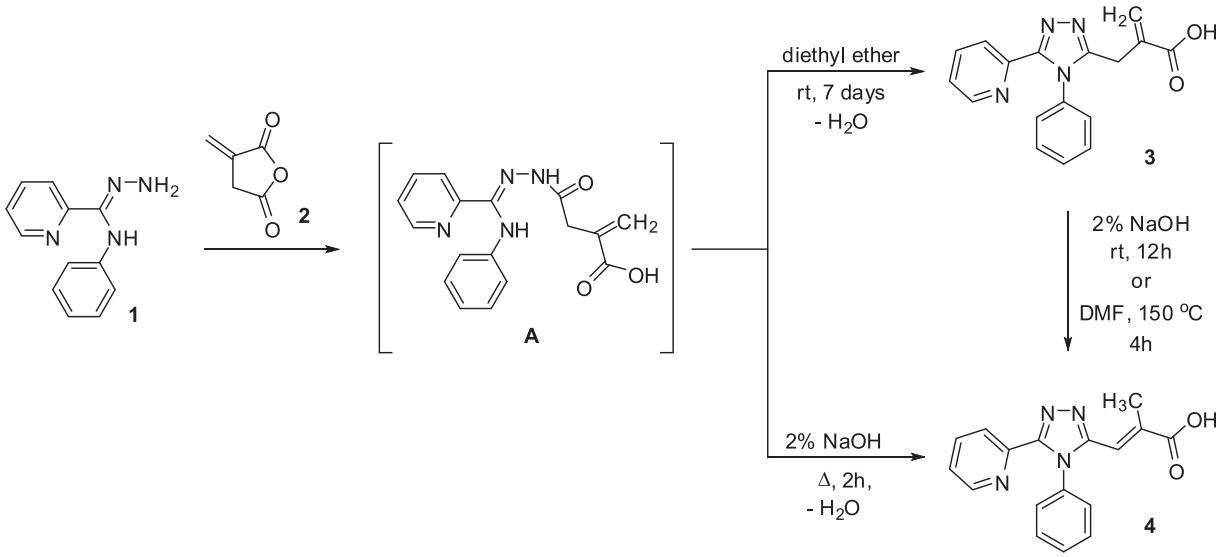

Scheme 1. The reaction of *N*-phenyl(pyridine-2-yl)carbohydrazonamide (**1**) with itaconic anhydride (**2**).

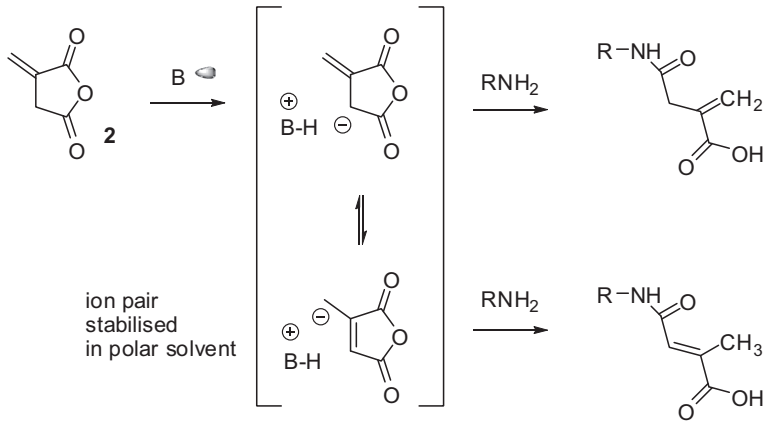

Scheme 2. Reactivity of itaconic anhydride.

by varying organic solvents and reaction temperature were not successful due to formation of intractable mixtures of products. We succeeded, however, in obtaining the compound **4** in 75% yield from hydrazonamide **1** and itaconic anhydride **2** by the treatment of the crude intermediate **A**, initially formed in diethyl ether solution, with aqueous NaOH solution at reflux (Scheme 1).

The molecular structures of the newly prepared 1,2,4-triazole derivatives **3** and **4** were confirmed unambiguously by ^{1}H and ^{13}C NMR spectroscopic data including $^{1}H—^{13}C$ HSQC and HMBC correlation studies (Supplementary material) as well as by single crystal X-ray diffraction analysis (Figs. 1–6).

The experimental NMR spectra of the compounds **3** and **4** were compared with the calculated proton and carbon shifts obtained by means of the density functional calculations (Table 1). The allyl group of **3** was similarly described by the all tested models, however the Empirical Density Functional 1 (EDF1) method exhibited the lowest root-mean-square deviation (RMSD) of 0.38 ppm. On the contrary, in the case of the ^{1}H and ^{13}C NMR spectra of **4** the B3LYP and EDF2 models gave considerably better results than EDF1, especially for the carbon atoms. It is worth noting that the most accurate ^{13}C NMR prediction was obtained using the corrected B3LYP method which accounts local environment in addition to the directly calculated shifts (RMSD = 3.16 ppm) [18].

3.2. X-ray crystallography

Compounds **3** and **4** crystallize in the monoclinic space group $P2_1/n$ and *Pn*, respectively. An independent part of the unit cell consists of one molecule of 2-methylene-4-oxo-4-(2-((phenylamino)(pyridin-2-yl)methylene)hydrazinyl)butanoic acid in the former case, and 2-((4-phenyl-5-(pyridin-2-yl)-4*H*-1,2,4-triazol-3-yl)methyl) acrylic acid with water molecule (1:1), in the latter one.

The molecule of **3** is composed of the central 1,2,4-triazole ring, substituted at the C3, N4 and C5 atoms by 2-methacrylic acid, phenyl and 2-pyridyl groups, respectively (Fig. 1). The interatomic distances within the triazole ring are not equal (Table 3) but comparable with those observed for the other closely related 1,2,4-triazole derivatives [20,21]. The N1—C5, N2—C3 bonds, with the interatomic distances of 1.315(2) and 1.307(2) Å, display a double-bond character, whereas those of C3—N4 and N4—C5 ones [1.374(2) and 1.375(2) Å] are of intermediate character. The central heterocyclic ring in **3** is planar but not coplanar with its substituents. The pyridyl and phenyl rings are twisted about the external bond to the 1,2,4-triazole ring; the angles between the least-squares planes through the pyridyl/phenyl and triazole rings are 18.55(7)° and 63.66(5)°, respectively. The planes through the pyridyl and benzene rings form a dihedral angle of 56.20(5)°. As in the

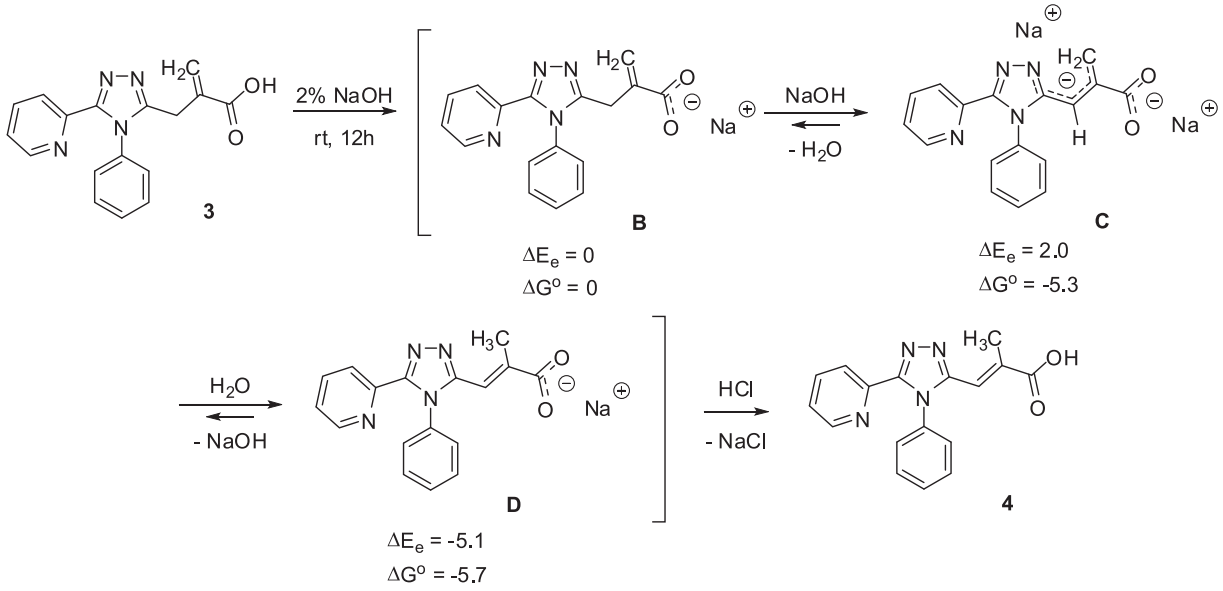

Scheme 3. The base promoted 1,3-proton shift of 2-((4-phenyl-5-(pyridin-2-yl)-4*H*-1,2,4-triazol-3-yl)methyl)acrylic acid (**3**) with the relative electronic energy (ΔE_e, kcal/mol) and Gibbs free energy (ΔG°, kcal/mol, 298.15 K) profiles calculated with B3LYP 6-31+G* method using SM8 water solvation model [19].

parent itaconic acid [22] the carboxyl O1 atom in **3** is *cisoidally* oriented with respect to the terminal =CH_2 group. It is worth noting, that the same orientation was observed in the crystal structures of most C^3-unsubstituted 2-methacrylic acid derivatives, reported so far [23]. However, contrary to the free acid, a significant deviation from planarity is observed for the methacrylic system in **3** as indicated from the torsion angles O1—C1—C2—C4 and O1—C1—C2—C6, being of 160.0(1)° and −25.4(2)°, respectively. This might be caused by steric hindrance between the carboxyl and triazole moieties, which seems to be supported by relative widening of O1-C1-C2 angle (by about 1.3°). The C1—O2 and C2—C6 distances [1.213(2) and 1.315(2) Å] are in good agreement with the localized double bond lengths, whereas the C1—C2 distance [1.493(2) Å] confirms the presence of unconjugated Csp^2—COOH single bond [23,24].

Geometry of **4** displays significant similarities to **3**, except obvious hydrogen transfer from CH_2 fragment (at C4 carbon atom) to CH_2 group (at C6 carbon atom), what involves appropriate changes of hybridizations and methyl group formation (Fig. 2). Therefore, for instance, in both systems the pyridine and benzene rings are twisted in respect to the 1,2,4-triazole ring to similar extent: the angles between the best planes of the pyridine or benzene rings and triazole fragment are 23.90° and 66.86°, respectively. The bond lengths in the methacrylic moiety are within normal ranges and are comparable to those observed for closely related mesaconic acid [25]. The relative orientation of carboxyl C1 and triazole C3 atoms indicate *transoid* conformer with the carboxyl group twisted from the plane of C4=C2(C6)—C1 atoms by the angle of 28.75(5)°.

The most characteristic feature of crystal **3** is the presence of catemers formed by translation related molecules propagated along the *a* axis (Fig. 3). Within each chain 'head-to-tail' oriented molecules are linked by the O1—H1o···N3$^{(i)}$ and C11—H11···O2$^{(ii)}$ hydrogen bonds (symmetry codes as in Table 4) giving $R_2^2(7)$ rings. Furthermore, the molecules belonging to the adjacent antiparallel chains are connected by an extended net of weak C—H···O/N hydrogen bonds between the atoms of 2-methacrylic system as well as the pyridyl/phenyl and triazole rings giving rise to complex 3D supramolecular architecture (Fig. 5). The pattern of interactions in (*E*)-2-methyl-3-(4-phenyl-5-(pyridin-2-yl)-4*H*-1,2,4-triazol-3-yl)acrylic acid (**4**) is totally different. The co-crystallizing water molecule behaves as a structural gluing factor [26,27]. It links three molecules together and serves as the hydrogen bond acceptor to hydroxyl group at carboxylic fragment (O1···O1w$^{(ii)}$ [2.515 Å]) of one molecule and hydrogen bond donor to carbonyl group (O1w···O2 [2.820 Å]) and nitrogen atom at triazole ring (O1w···N1$^{(viii)}$ [2.780 Å]) of two other molecules, as shown in Figs. 4 and 6.

3.3. Theoretical studies

The observed **3** → **4** isomerization in aqueous NaOH solution corresponds to numerous base-promoted 1,3-proton shifts described in the literature [28–30] including isomerisation of itaconic acid to mesaconic acid [31]. In order to elucidate the chemical mechanism, which leads to rearranged isomeric triazole derivative **4**, we have performed B3LYP/6-31+G* DFT calculations with use of SM8 water solvation model [19]. As depicted in Scheme 3, the proposed reaction sequence is comprised of the initial exothermic abstraction of the acidic methylene proton (ΔG° = −5.3 kcal/mol) that leads to the formation of carbanion **C** and the subsequent hydrolysis giving rise to the formation of salt **D** (ΔG° = −5.7 kcal/mol). The following neutralization of carboxylate function with diluted hydrochloric acid provides the isomerized alkene derivative **4**. It is worth noting that weaker bases such as triethylamine or pyridine were ineffective in catalyzing the conversion of **3** to **4**.

From a theoretical point of view, however, the most interesting is the less frequently investigated [32] neutral thermal rearrangement of **3** to **4** observed in DMF solution at 150°C. In this study we have considered three possible mechanisms of 1,3-proton shifts presented in Scheme 4.

First, the direct C → C proton transfer via transition state **TS1** leading to *cis*-olefin **E**. The activation energy of the rearrangement **3** → **E** via direct intramolecular proton transfer is very high (ΔE_e = 73.2 kcal/mol), and therefore, it should not occur. In fact, the *cis*-isomer **E** was not detected in NMR spectrum of the crude reaction product.

Second, the two step mechanism which consists in the initial C → N 1,3-proton shift via transition state **TS2** (ΔE_e = 73.9 kcal/mol) furnishing the dearomatized triazole **F**, which is followed by N → C 1,5-proton shift via transition state **TS3** (ΔE_e = 36.2 kcal/mol) that leads to the final product **4**. Although the activation energy of C → N 1,3 proton transfer is slightly lower than that

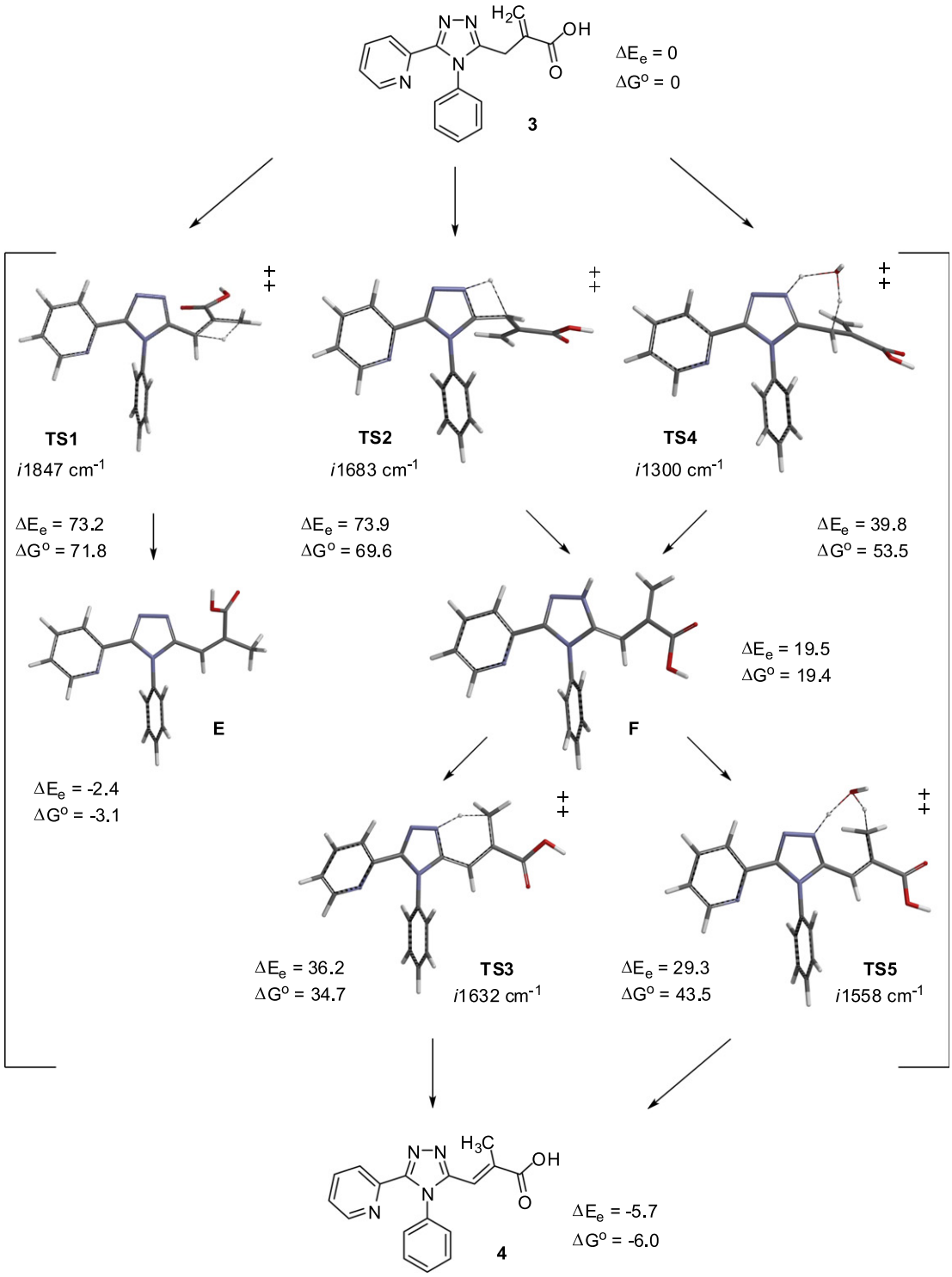

Scheme 4. Thermal 1,3-proton shift reaction with the relative electronic energy (ΔE_e, kcal/mol) and Gibbs free energy ($\Delta G°$, kcal/mol, 423.15 K) profiles calculated with B3LYP 6-31+G* method using SM8 DMF solvation model [19].

calculated for direct C → C transfer, it is still prohibitive, and therefore, the formation of **F** should be considered an unfavorable process.

Third plausible mechanism, i.e. water-mediated double-proton transfer reaction is based on interactions between the solute and the solvent molecules. The thermal rearrangement of **3** to **4** is carried out in the reagent grade DMF which contains a considerable amount of water, hence, the "water-relay" mechanism cannot be excluded. According to this model, the nucleophilic water can accept a proton from the donor site of the solute molecule and transfer a different proton to the acceptor site, which often results in significant lowering of the energy barrier in proton transfer-related reactions, including various 1,3-proton shifts [33–40]. As shown in Scheme 4, upon addition of water molecule the energy barrier of the rearrangement of **3** → **F** is lower by 34.1 kcal/mol than that for the direct C → N 1,3-proton shift. The transition state **TS4** is characterized by ΔE_e = 39.8 kcal/mol and a single imaginary frequency (i1300 cm^{-1}) referring to C—H—O bond breakage and

N—H—O bond formation. The C—H and N—H atom distances are 1.428 and 1.055 Å, while the O—H atoms are separated by 1.241 and 1.689 Å, respectively.

Interestingly, the subsequent relayed N → C 1,5-proton shift in **F** leading to the final product **4** via transition state **TS5** is energetically more favorable than the alternative direct shift via **TS3** (ΔE_e = 29.3 vs 36.2 kcal/mol). However, the "catalytic" effect of relay is significantly reduced due to entropic cost associated with constructing the relay pathway with aid of an supramolecule comprising eight-membered ring. As a result water assisted **F** → **4** transformation is unfavorable thermodynamically (ΔG° = 43.5 kcal/mol vs 34.7 kcal/mol).

From the above calculations one may infer that the thermal isomerization of **3** to **4** proceeds via a stepwise mechanism involving water-assisted C → N 1,3-proton shift and the direct N → C 1,5 proton shift, i.e. according to the following pathway: **3** → **TS4** → **F** → **TS3** → **4**.

3.4. Antibacterial activity of compounds *3*, *4* in vitro

New synthesized compounds were evaluated for their antibacterial activity using a broth microdilution method. Compound **3** was shown to be effective against *S. lutea* and *E. faecalis* ATCC 29212 (MIC_{50} 100 μg/mL) as well as against *Y. enterocolitica* O3, *Nocardia spp* and *C. albicans* at a concentration of 250 μg/mL. The derivative **4** inhibited growth of *Y. enterocolitica* O3, *M. smegmatis*, *Nocardia* and *C. albicans* at the concentration 250 μg/mL. The examined compounds did not inhibit the growth of *E. coli* ATCC 25922, *S. aureus* ATCC 25923 and *P. aeruginosa* ATCC 27853.

4. Conclusion

The reaction of *N*-phenyl-(pyridin-2-yl)carbohydrazonamide with itaconic anhydride appears to be useful for preparation of novel 1,2,4-triazole-containing analogues of alkenoic acids with antimicrobial activity. Thus, depending on the conditions, either 2-((4-phenyl-5-(pyridin-2-yl)-4*H*-1,2,4-triazol-3-yl)methyl)acrylic acid (**3**) or (*E*)-2-methyl-3(4-phenyl-5-(pyridine-2-yl)-4*H*-1,2,4-triazol-3-yl)acrylic acid (**4**) could be obtained in 15% and 75% yield, respectively. It was proved that the terminal alkene derivative (**3**) undergoes a facile isomerization of into the more thermodynamically stable internal alkene (**4**). DFT B3LYP studies combined with SM8 (H_2O, DMF) solvation models revealed that the base-catalyzed isomerization proceeds with initial exothermic abstraction of the acidic methylene proton while the thermal 1,3-proton shift involves a stepwise mechanism comprising the water-assisted C → N 1,3-proton shift and the direct N → C 1,5 proton shift.

Acknowledgements

Work supported in part by a grant from the Polish Ministry of Science and Higher Education No. N N204 546839.

Appendix A. Supplementary material

Cartesian coordinates, computed electronic energies and Gibbs free energies for structures **3**, **4**, **B**, **C**, **D**, **E**, **F**, **TS1**-**5**; HSQC and HMBC NMR spectra of compound **4**. Crystallographic data for the structures reported in this paper have been deposited with the Cambridge Crystallographic Data Centre as supplementary publications Nos. CCDC-861928 (**3**) and CCDC-830714 (**4**). Copies of available materials can be obtained free of charge on application to CCDC, 12 Union Road, Cambridge CB2 1EZ, UK (fax: +44 1223 336 033; e-mail: data_request@ccdc.cam.ac.uk or www: http://www.ccdc.cam.ac.uk/data_request/cif). Supplementary data associated with this article can be found, in the online version, at http://dx.doi.org/10.1016/j.molstruc.2012.04.087.

References

[1] For recent comprehensive review see I.A. Al-Masoudi, Y.A. Al-Soud, N.J. Al-Salihi, N.A. Al-Masoudi, Chem. Heterocycl. Compd. 42 (2006) 1377.
[2] H. Gerson, M.W. McNeil, R. Parmegiani, P.K. Godfrey, J.M. Baricko, Antimicrob. Agents Chemother. 4 (1973) 435.
[3] S. Omura, M. Katagiri, J. Awaya, I. Omezawa, N. Oi, M. Mizagushi, Antimicrob. Agents Chemother. 6 (1974) 207.
[4] R.A. Scherrer, US Patent 4048323, 1977.
[5] B. Narasimhan, D. Belasre, D. Pharande, V. Mourya, A. Dhake, Eur. J. Med. Chem. 39 (2004) 827.
[6] A. Spasov, E. Golovinskii, Zhurnal Obshchei Khimii 32 (1962) 3394.
[7] B. Modzelewska-Banachiewicz, J. Banachiewicz, A. Chodkowska, E. Jagiell-Wojtowicz, L. Mazur, Eur. J. Med. Chem. 39 (2004) 873.
[8] B. Modzelewska-Banachiewicz, B. Michalec, T. Kaminska, L. Mazur, A.E. Koziol, J. Banachiewicz, M. Ucherek, M. Kandefer-Szerszen, Monatsh Chem. 140 (2009) 439.
[9] M. Ziegler-Borowska, M. Ucherek, J. Kutkowska, L. Mazur, B. Modzelewska-Banachiewicz, D. Kedziera, A. Kaczmarek-Kedziera, Tetrahedron Lett. 51 (2010) 2951.
[10] A.V. Galanti, B.T. Keen, R.H. Pater, D.A. Scola, J. Polym. Sci. 19 (1981) 2243.
[11] M.C. Galanti, A.V. Galanti, J. Org. Chem. 47 (1982) 1572.
[12] CrysAlis RED, Oxford Diffraction Ltd., Version 1.171.33. Empirical absorption correction using spherical harmonics, implemented in SCALE3 ABSPACK scaling algorithm.
[13] CrysAlis CCD, Oxford Diffraction Ltd., Version 1.171.33; CrysAlis RED, Oxford Diffraction Ltd., Version 1.171.33.
[14] G.M. Sheldrick, Acta Crystallogr. A 46 (1990) 467.
[15] G.M. Sheldrick, SHELXL93. Program for the Refinement of Crystal Structures. Univ. of Göttingen, Germany, 1993.
[16] International Tables for Crystallography, in: A.J.C. Wilson (Ed.), Kluwer, Dordrecht, 1992 (vol. C).
[17] C.F. Macrae, P.R. Edgington, P. McCabe, E. Pidcock, G.P. Shields, R. Taylor, M. Towler, J. van de Streek, J. Appl. Cryst. 39 (2006) 453.
[18] Spartan '08, Wavefunction, inc., 18401 Von Karman Ave., Suite 370, Irvine, CA 92612, USA. http://www.wavefun.com.
[19] A.V. Marenich, R.M. Olson, C.P. Kelly, C.J. Cramer, D.G. Truhlar, J. Chem. Theory Comput. 3 (2007) 2011.
[20] L. Mazur, A.E. Koziol, B. Modzelewska-Banachiewicz, Acta Cryst. C 64 (2008) o574.
[21] L. Mazur, A.E. Koziol, B. Modzelewska-Banachiewicz, M. Ucherek, M. Zimecki, J. Artym, J. Chem. Cryst. 41 (2011) 880.
[22] R.L. Harlow, C.E. Pfluger, Acta Cryst. B 29 (1973) 2965.
[23] Cambridge Structural Database (CSD) F.H. Allen, Acta Cryst. B 58 (2002) 380.
[24] F.H. Allen, O. Kennard, D.G. Watson, L. Brammer, A.G. Orpen, R. Taylor, J. Chem. Soc., Perkin Trans. 2 (1987) S1.
[25] M.P. Gupta, S.R.P. Yadav, Acta Cryst. B 28 (1972) 2682.
[26] T.M. Krygowski, S.J. Grabowski, J. Konarski, Tetrahedron 54 (1998) 11311.
[27] S. Witkowski, R. Annulewicz-Ostrowska, T.M. Krygowski, Polish J. Chem. 75 (2001) 883.
[28] A.R. Katritzky, J. Li, N. Malhotra, Liebigs. Ann. Chem. (1992) 843.
[29] V.A. Soloshonok, V.P. Kukhar, Tetrahedron 52 (1996) 6953.
[30] P. Nagy, H. Ueki, D.O. Berbasov, V.A. Soloshonok, J. Fluor. Chem. 129 (2008) 409.
[31] E.R.H. Jones, G.H. Witham, M.C. Whiting, J. Chem. Soc. (1954) 1865.
[32] M. Yasumoto, H. Ueki, V.A. Soloshonok, J. Fluor. Chem. 128 (2007) 736.
[33] X.-C. Wang, J. Nicholas, J. Phys. Chem. 95 (1991) 10419.
[34] C. Adamo, M. Brossi, V. Barone, J. Comput. Chem. 18 (1997) 1993.
[35] L. Gorb, J. Leszczynski, J. Am. Chem. Soc. 120 (1998) 5024.
[36] G.M. Chaban, M.S. Gordon, J. Phys. Chem. A 103 (1999) 185.
[37] M.K. Schukla, J. Leszczyński, THEOCHEM 529 (2000) 99.
[38] N. Markowa, V. Enchev, THEOCHEM 679 (2004) 195.
[39] V. Enchev, N. Markowa, S. Angelova, J. Phys. Chem. A 109 (2005) 8904.
[40] Y. Yang, Q. Cui, J. Phys. Chem. B 113 (2009) 4930.